

Atlas of expression of acyl CoA binding protein/diazepam binding inhibitor (ACBP/DBI) in human and mouse

Sijing Li et al.

Legends to Supplemental Figures

Fig. S1. Immunoblotting of ACBP/DBI in mouse tissues. The differential expression of ACBP/DBI was assessed by immunoblotting analysis of tissue samples from female and male mice (Quantification of these results referred to Fig. 2). LC samples represent loading controls (LC2: 2μg; LC20: 20μg). n=5 per condition.

Fig. S2. Gene expression profile of ACBP/DBI at the single-cell level across distinct human tissues. Dot plots illustrating the single-cell expression of ACBP/DBI in human tissues, including adrenal gland (A), axilla (B), bladder organ (C), gallbladder (D), blood (E), bone marrow (F), breast (G), embryo (H), endocrine gland (I), esophagogastric junction (J), eye (K), esophagus (L), exocrine gland (M), and Fallopian tube (N). The dot color indicates scaled ACBP/DBI expression ($\ln(\text{CPTT}+1)$). The dot size represents ACBP/DBI expressed in cells (% tissue Composition). The single-cell RNA data were obtained from CZ CELLxGENE database (<https://cellxgene.cziscience.com/>).

Fig. S3. Gene expression profile of ACBP/DBI at the single-cell level across distinct human tissues. Dot plots showing the single-cell expression of ACBP/DBI in human tissues, including intestine (A), lamina propria (B), omentum (C), lymph node (D), mucosa (E), musculature (F), nose (G), ovary (H), pancreas (I), placenta (J), pleura (K), pleural fluid (L), and prostate gland (M). The dot color indicates scaled ACBP/DBI expression ($\ln(\text{CPTT}+1)$). The dot size represents ACBP/DBI expressed in cells (% tissue Composition). The single-cell RNA data were obtained from CZ CELLxGENE database (<https://cellxgene.cziscience.com/>). Note that parenchymatous cell types are marked in red, while myeloid and glial cell types are marked in blue.

Fig. S4. Gene expression profile of ACBP/DBI at the single-cell level across distinct human tissues. Dot plots showing the single-cell expression of ACBP/DBI in human tissues, including scalp (A), saliva (B), stomach (C), spleen (D), spinal cord (E), small intestine (F), testis (G), tongue (H), uterus (I), vasculature (J), and yolk sac (K). The dot color indicates scaled ACBP/DBI expression ($\ln(\text{CPTT}+1)$). The dot size represents ACBP/DBI expressed in cells (% tissue Composition). The single-cell RNA data were

obtained from CZ CELLxGENE database (<https://cellxgene.cziscience.com/>). Note that parenchymatous cell types are marked in red, while myeloid and glial cell types are marked in blue.

Fig. S5. Gene expression profile of *Acbp/Dbi* at the single-cell level across distinct mouse tissues. Dot plots show the single-cell expression of ACBP/DBI in mouse tissues, including adipose tissue (A), bone marrow (B), brain (C), embryo (D), endocrine gland (E), exocrine gland (F), and eye (G). The dot color indicates scaled ACBP/DBI expression ($\ln(\text{CPTT}+1)$). The dot size represents ACBP/DBI expressed in cells (% , tissue Composition). The single-cell RNA data was obtained from CZ CELLxGENE database (<https://cellxgene.cziscience.com/>). Note that parenchymatous cell types are marked in red, while myeloid and glial cell types are marked in blue.

Fig. S6. Gene expression profile of *Acbp/Dbi* at the single-cell level across distinct mouse tissues. Dot plots display the single-cell expression of *Acbp/Dbi* in heart (A), large intestine (B), kidney (C), liver (D), musculature (E), ovary (F), and lung (G). The dot color indicates scaled ACBP/DBI expression ($\ln(\text{CPTT}+1)$). The dot size represents ACBP/DBI expressed in cells (% , tissue Composition). The single-cell RNA data were obtained from CZ CELLxGENE database (<https://cellxgene.cziscience.com/>). Note that parenchymatous cell types are marked in red, while myeloid and glial cell types are marked in blue.

Fig. S7. Gene expression profile of *Acbp/Dbi* at the single-cell level across distinct mouse tissues. Dot plots display the single-cell expression of *Acbp/Dbi* in pancreas (A), prostate gland (B), skin of body (C), spleen (D), testis (E), tongue (F), urethra (G), vasculature (H), and urinary bladder (I). The dot color indicates scaled ACBP/DBI expression ($\ln(\text{CPTT}+1)$). The dot size represents ACBP/DBI expressed in cells (% , tissue Composition). The single-cell RNA data were obtained from CZ CELLxGENE database (<https://cellxgene.cziscience.com/>). Note that parenchymatous cell types are marked in red, while myeloid and glial cell types are marked in blue.

Fig. S8. Co-regulation of *Acbp/Dbi* and its co-expressed genes by *Acbp/Dbi* inhibition. The heatmap displays the alterations of ACBP/DBI and its co-expressed genes upon the inhibition of ACBP/DBI (ACBP/DBI knockout, anti-ACBP, and KLH-ACBP) in mouse liver tissues. The RNA-seq data were obtained from GEO datasets (<https://www.ncbi.nlm.nih.gov/geo/>). *P* values were calculated using R package “DEseq2”.

Fig. S9. Correlations of the transcription factors upstream of ACBP/DBI and ACBP/DBI co-expression network. The heatmap displays the correlations between the predicted 71 high-coincidence ACBP/DBI-regulating transcription factors and ACBP/DBI co-expression network (ACBP/DBI as well as its co-expressed genes) in all the mouse tissues (referred to Fig.5). Correlation analyses were performed using Spearman's correlation test.

Fig. S10. Post-transcriptional and post-translational factors affecting ACBP/DBI. (A) The predicted microRNAs targeting ACBP/DBI by more than 2 datasets conserved in human and mouse. (B) Differential expression of ACBP/DBI-targeting microRNAs between tumors (T) and non-tumor (NT) tissues when available in TCGA datasets. (C) Spearman's correlation Rho values between ACBP/DBI and microRNAs targeting ACBP/DBI across cancers in TCGA. (D) Potential chemical modifications affecting ACBP/DBI mRNA conserved in human and mouse. The information was extracted from RM2Target database (<http://rm2target.canceromics.org/#/home>). (E) Post-translational modifications (PTM) of human and mouse ACBP/DBI protein. The sequence alignment view of ACBP/DBI indicates similarities and differences for PTMs (acetylation, phosphorylation, succinylation or ubiquitylation) in human and mouse. The PTM sites of ACBP/DBI residues are highlighted in red lower-case letters. This information was retrieved from the PhosphoSitePlus®v6.7.5 database (<https://www.phosphosite.org/homeAction>).

Supplemental figures

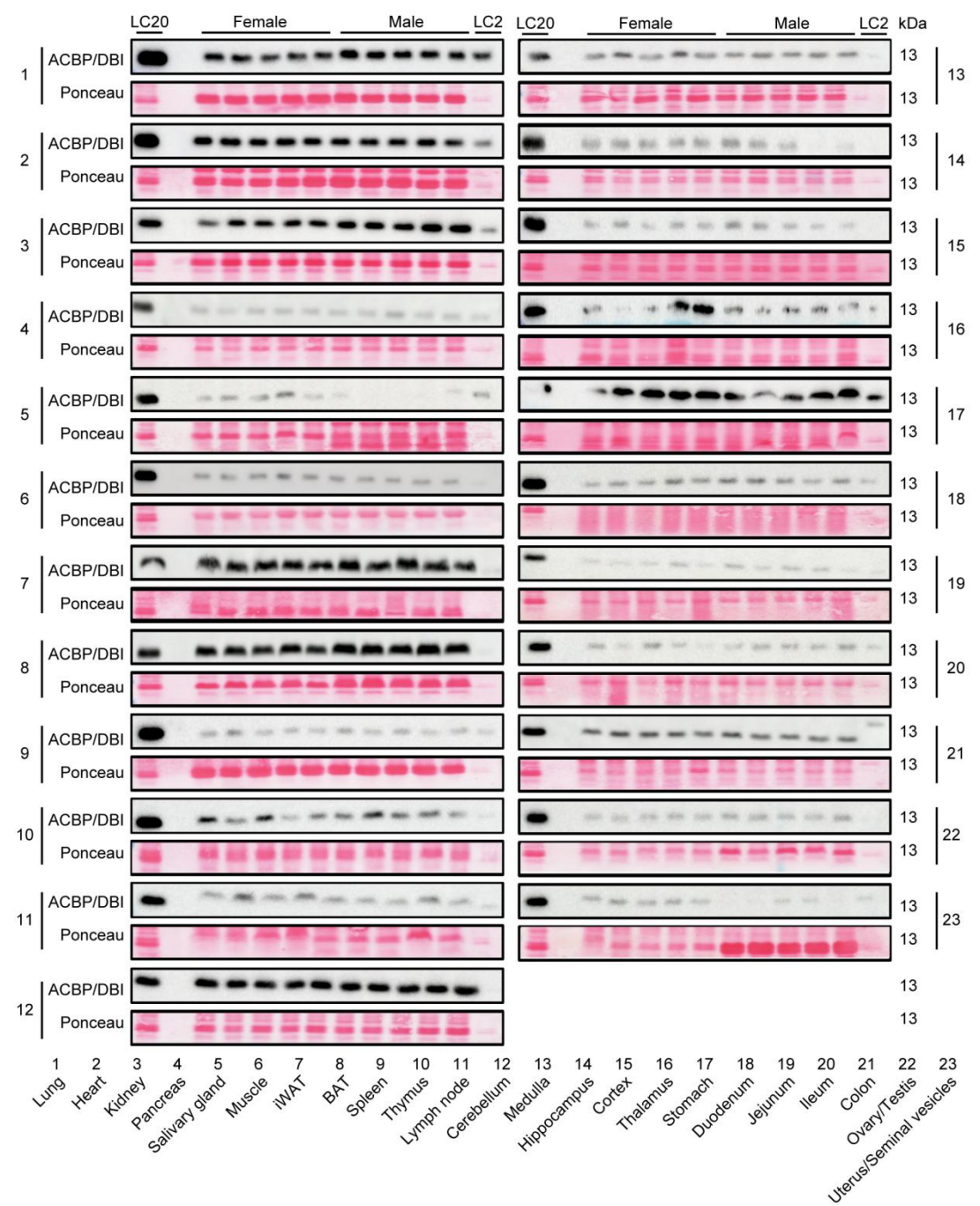


Fig. S1



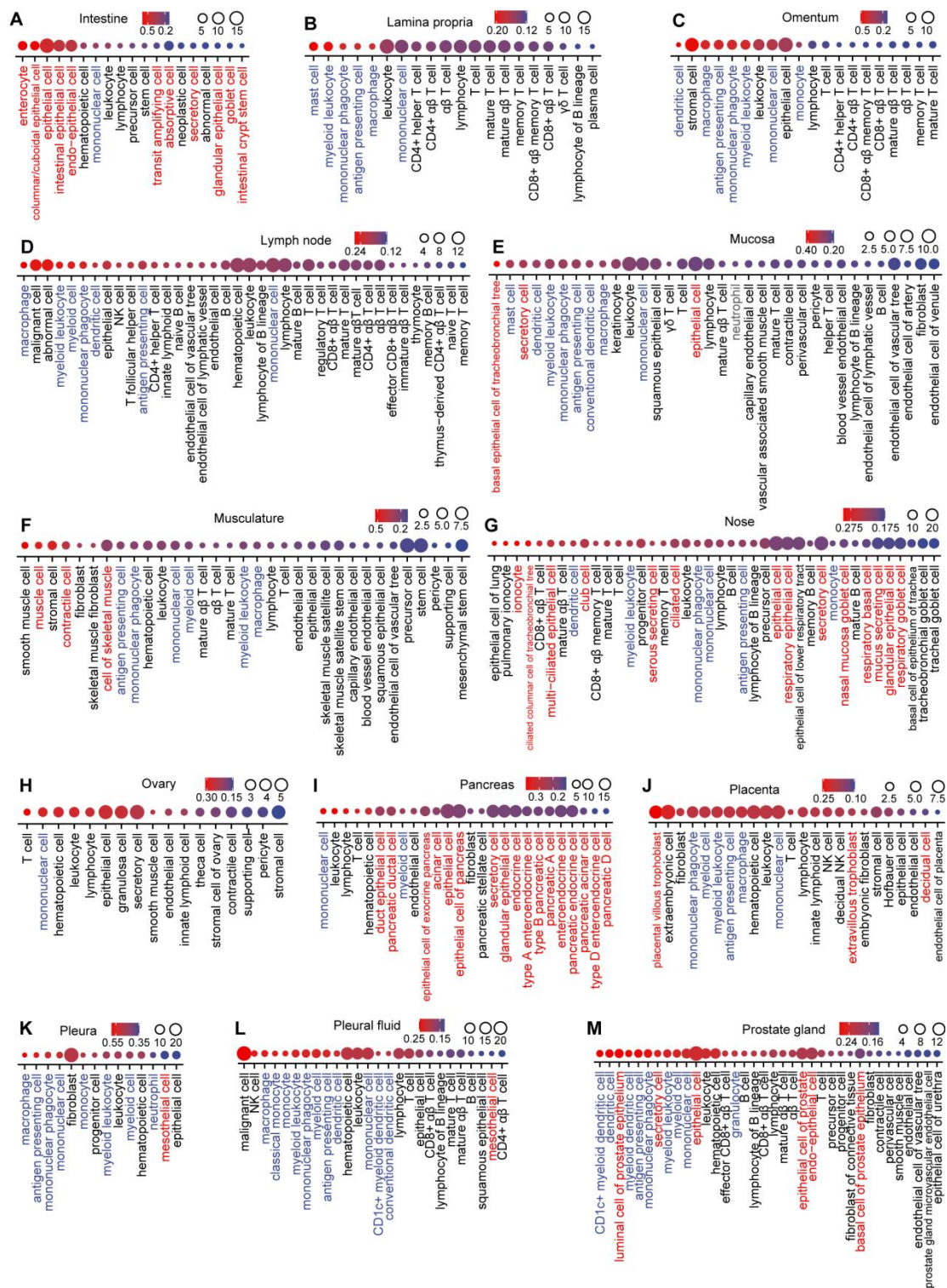


Fig. S3

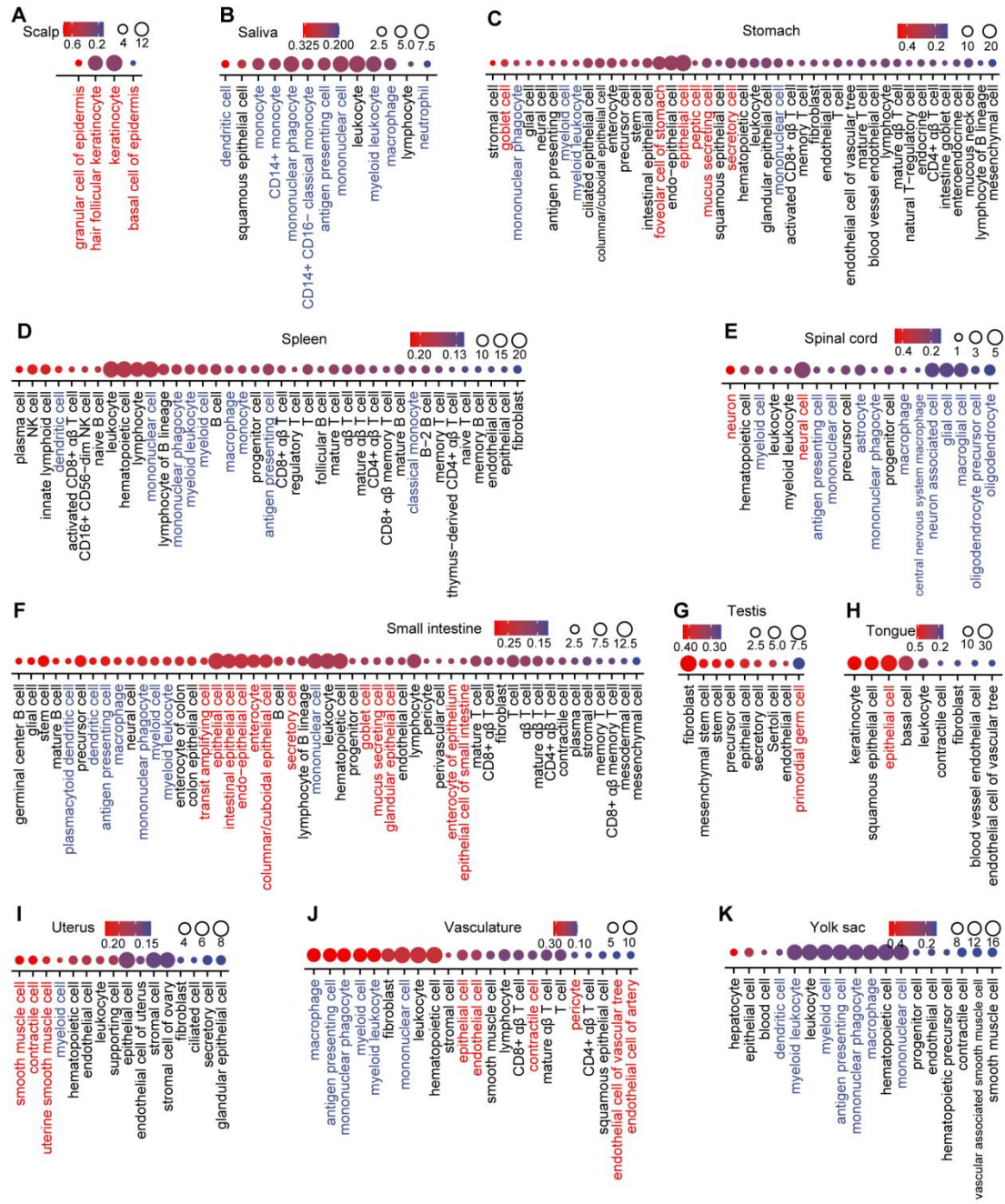


Fig. S4

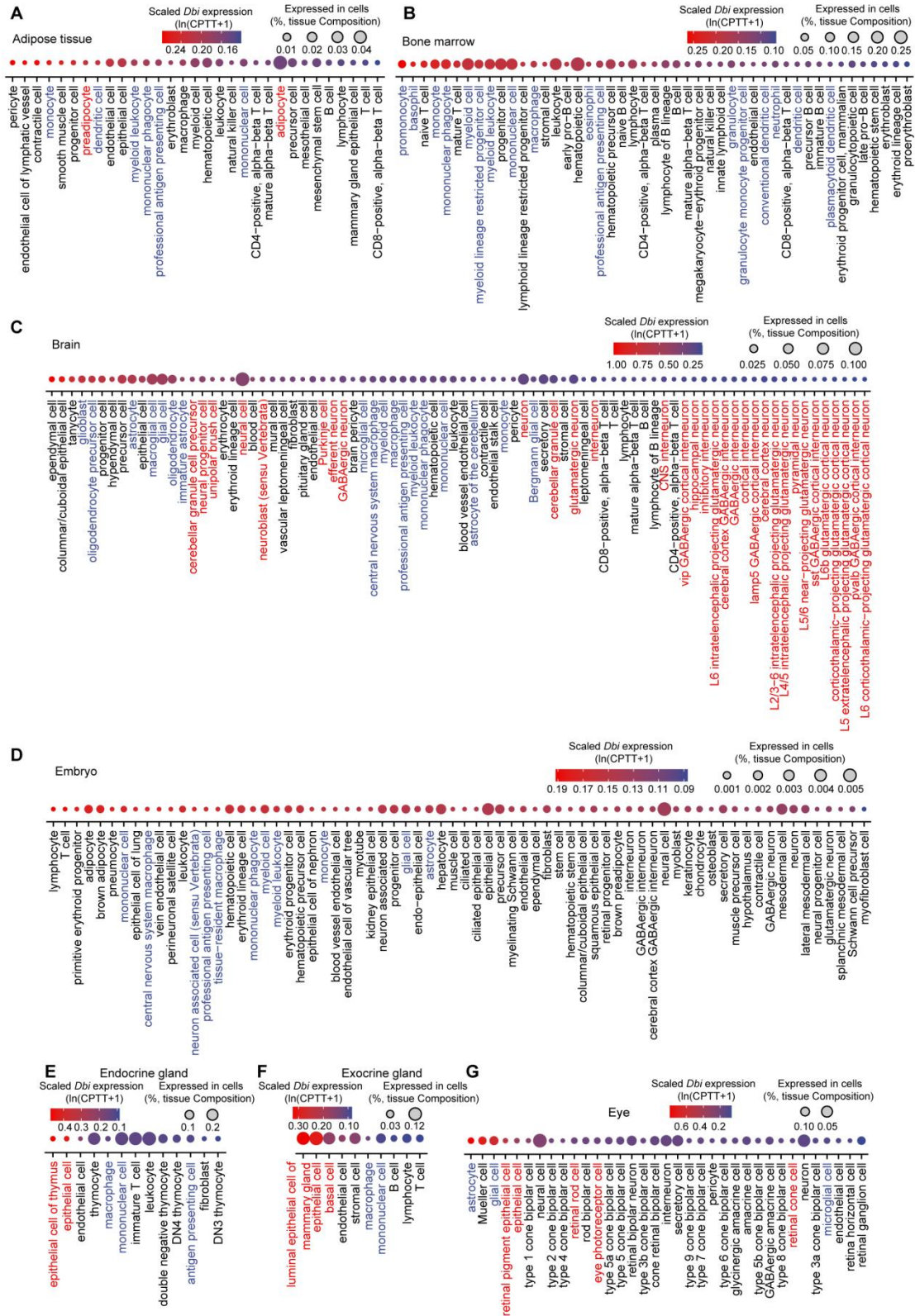


Fig. S5

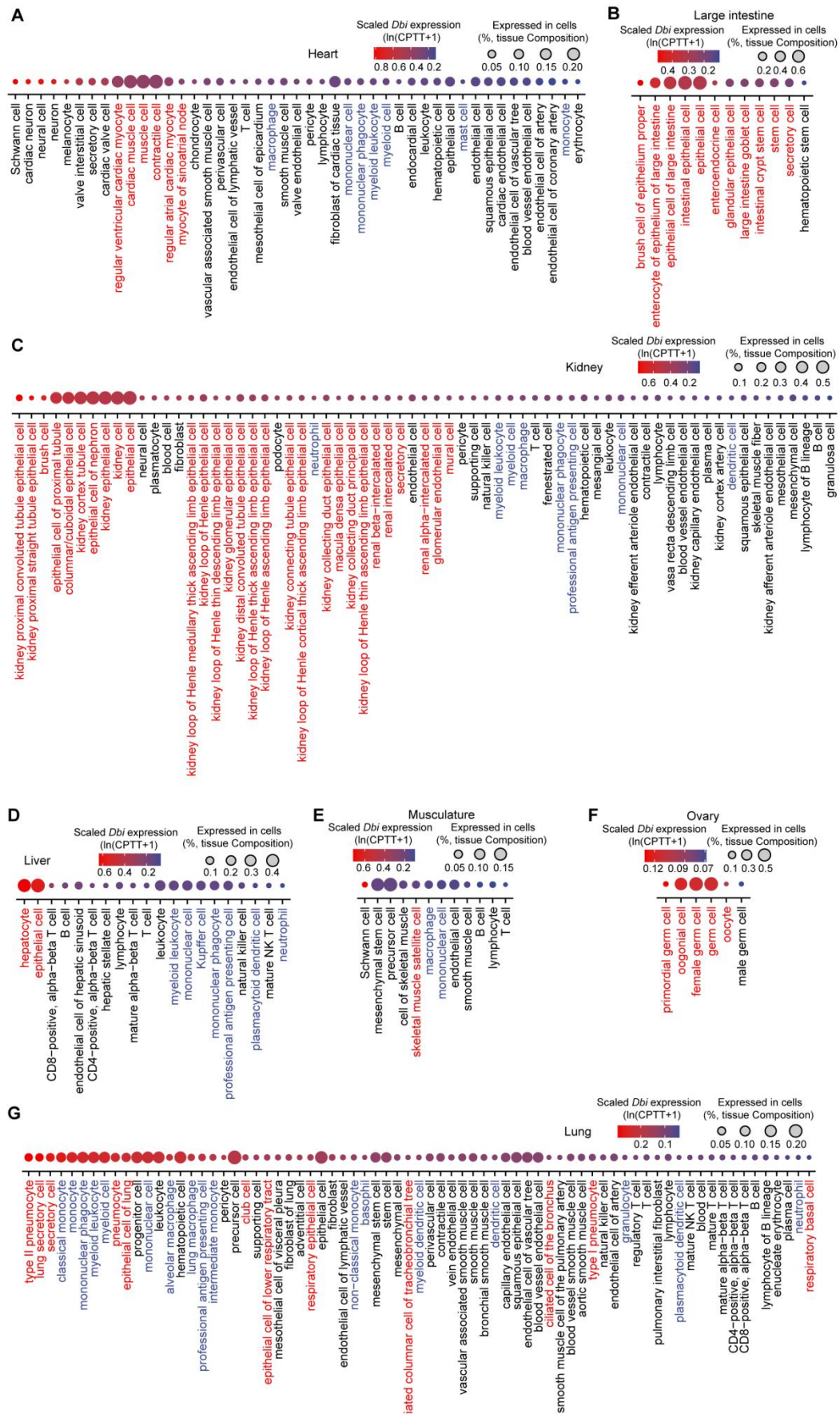


Fig. S6

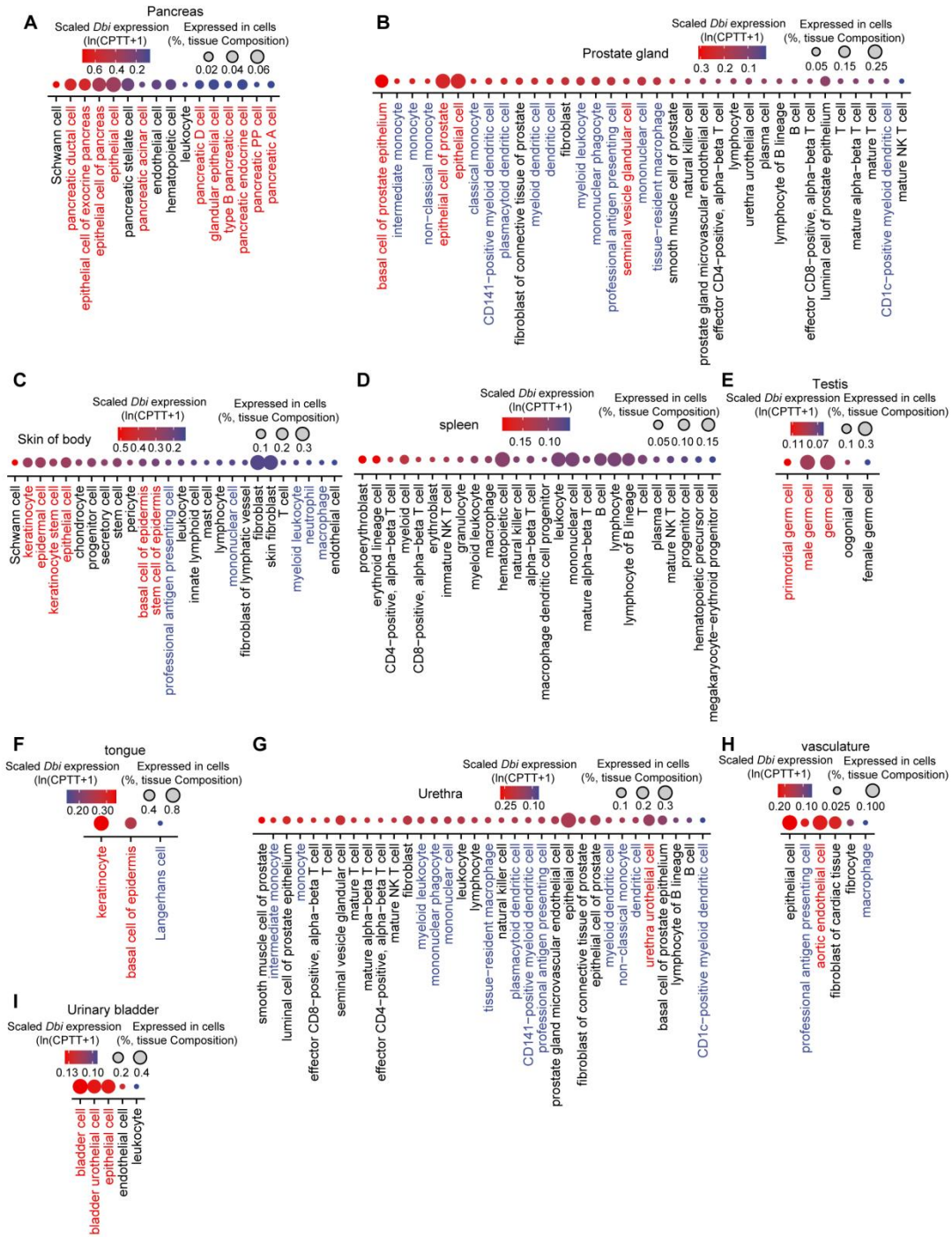


Fig. S7

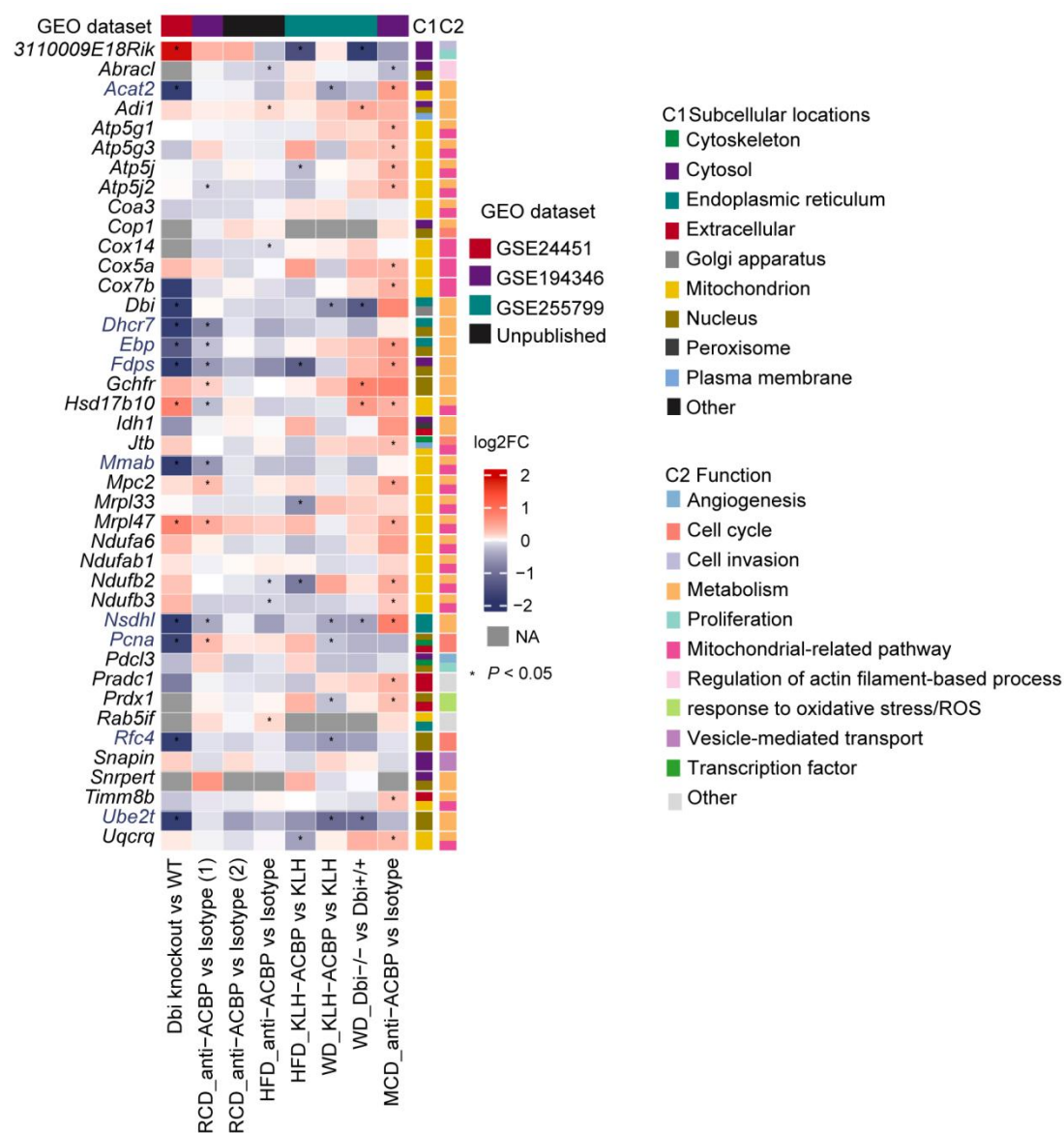


Fig. S8

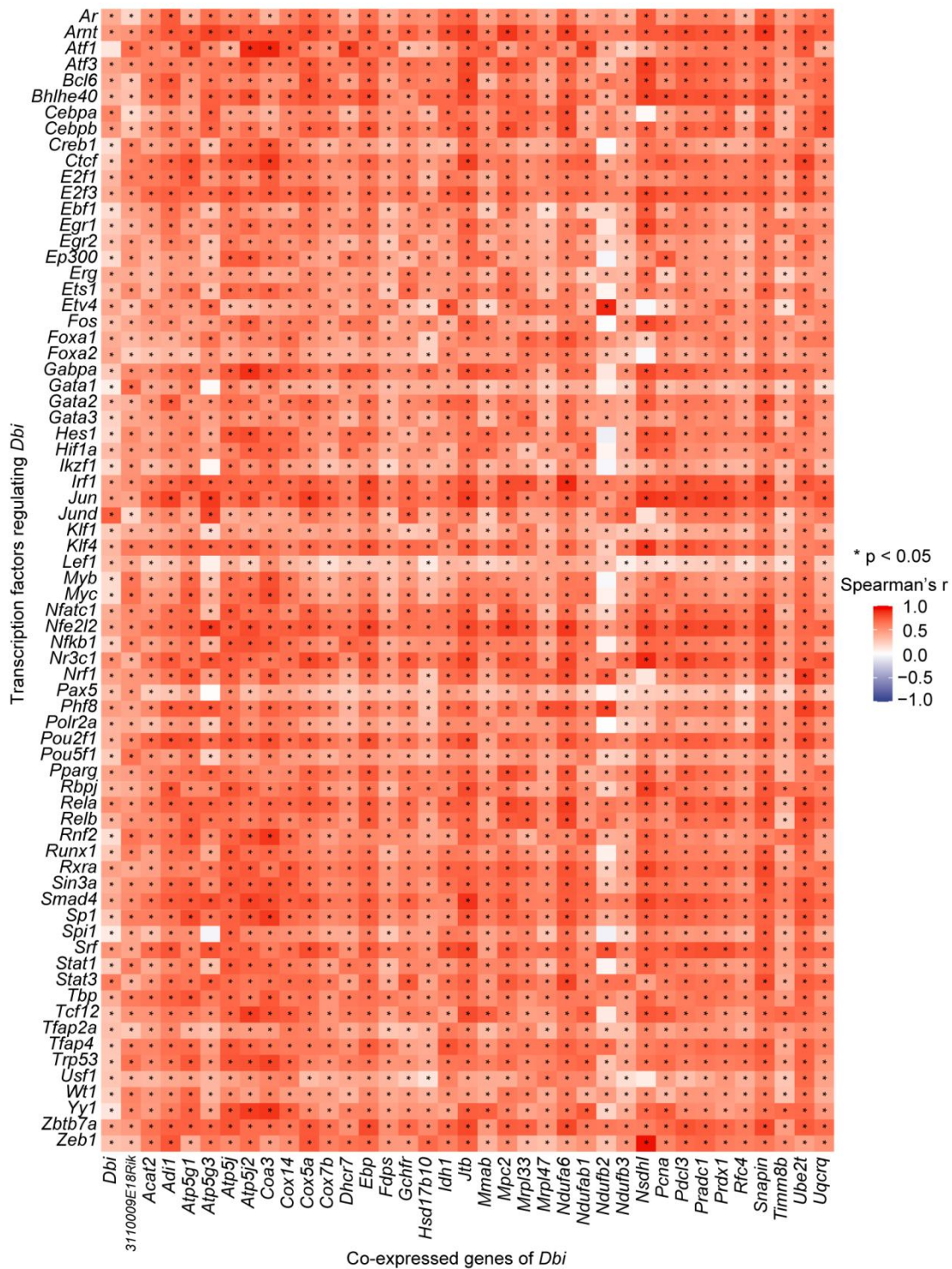


Fig. S9

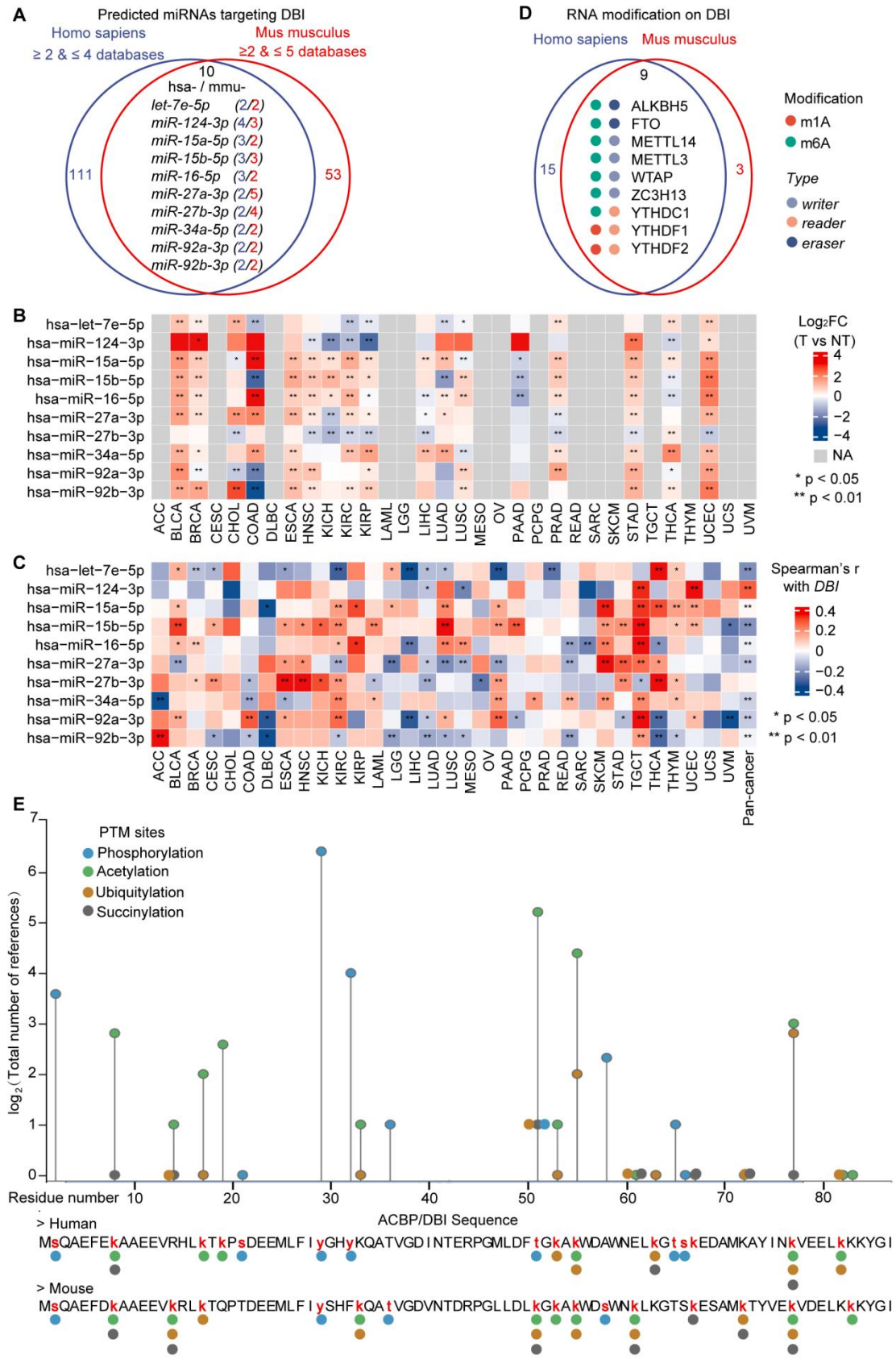


Fig. S10